Available online at www.sciencedirect.com
SCIENCE DIRECT®
Polyhedron 22 (2003) 3403–3411
POLYHEDRON
www.elsevier.com/locate/poly

Solid state structure and fluxionality in solution of $[H_4Ru_4(CO)_{11}L]$ ($L = P(C_6F_5)_3$, PMe_2Ph, $P(OMe)_3$ and $P(OEt)_3$): two different structures

M. Gabriela Ballinas-López, Efrén V. García-Báez [1], María J. Rosales-Hoz *

Departamento de Química, Centro de Investigación y de Estudios Avanzados del I.P.N., Apdo. Postal 14-740, 07000 México, DF, Mexico

Received 1 December 2002; accepted 15 August 2003

Abstract

The monosubstituted $[H_4Ru_4(CO)_{11}L]$ derivatives where $L = P(C_6F_5)_3$, PMe_2Ph, $P(OMe)_3$ and $P(OEt)_3$ (compounds **1** to **4**, respectively) were synthesized, the crystal structure of **1**, **2** and **4** were determined by X-ray diffraction (that of compound **3** had been determined previously but not fully reported so we obtained it again) and their dynamical behavior studied by ^1H, ^{31}P and ^{19}F NMR. The structures of compounds **1**, **3** and **4** show the common tetrahedral structure with four long (hydride bridged) and two short metal–metal bonds with the P-donor ligand transoid to an unbridged Ru–Ru bond. The structure of **2** is different since the M–M bonds to the Ru atom bonded to the phosphine, are all hydride-bridged. The variable temperature NMR studies of **1**, **2** and **3** show dynamical behaviour similar to what had been reported for compound **4**. However we propose that some of the structures involved in the equilibrium have the phosphorus substituent transoid to a bridged Ru–Ru bond.

Keywords: Solid state structures; Synthesis; Spectroscopic data; Polymetallic complexes

1. Introduction

The chemistry of the tetranuclear cluster $[H_4Ru_4(CO)_{12}]$ has been studied in some detail [1]. Reactions with phosphines and phosphites, alkynes and other derivatives have been carried out. The compound and some of its phosphine and phosphite derivatives, all tetrahedral 60-electron clusters, were tested as catalysts for polymerization of olefines [2] and reduction of aldehydes [3].

All these tetrahedral clusters show the well known pattern [4] of four long and two short metal–metal bonds. The long bonds are considered to be those bridged by the four hydride groups. There are two ways of accommodating four hydride ligands in a tetrahedral metal cluster. In one, the two short Ru–Ru bonds are opposite each other allowing a general *D2d* symmetry while in the other arrangement three of the long bonds span the tetrahedral edges adjacent to a single metal atom forming a metal core of *Cs* symmetry. Both arrangements have been observed in X-ray crystal structures of some of these derivatives [5–7] and this suggests a small energy difference between both structures as it is confirmed by the fluxional behavior shown by the hydrides in solution.

One of the studies reported on the dynamics of these derivatives is that carried out by Aime et al. [8]. In this study the authors observe, at low temperature, the presence of three isomers in the solution of the monosubstituted $[H_4Ru_4(CO)_{11}P(OEt)_3]$ and conclude that both hydride motion and CO exchange are taking place.

The availability of fast X-ray diffractometers allows the study of the effect of different substituents in the geometry of a particular cluster framework and this has been carried out for $[Os_3(CO)_{11}L]$ [9] and $[Rh_6(CO)_{15}L]$ [10], among other cluster compounds. Another study [11] has shown that the mechanism followed by substitution reactions of $[Ru_5C(CO)_{15}]$ is affected by electronic and steric characteristics of the entering ligand.

* Corresponding author. Tel.: +52-5-747-3800; fax: +52-5-747-7113.
E-mail address: mrosales@mail.cinvestav.mx (M.J. Rosales-Hoz).
[1] Present address: Departamento de Química, Unidad Profesional Interdisciplinaria de Biotecnología del I.P.N., Av. Acueducto s/n, Barrio La Laguna Ticomán, 07340 México, DF, Mexico.

0277-5387/$ - see front matter © 2003 Elsevier Ltd. All rights reserved.
doi:10.1016/j.poly.2003.08.009

As part of a study on the reactivity of substituted transition metal clusters, we have prepared four substituted derivatives of $[H_4Ru_4(CO)_{12}]$, namely $[H_4Ru_4(CO)_{11}L]$ with $L = P(C_6F_5)_3$, PMe_2Ph, $P(OMe_3)$ and $P(OEt)_3$ (compounds **1**–**4**, respectively). Compounds **3** and **4** had been previously prepared and spectroscopic data of compound **4** was reported by Aime et al. [8] while structural characterization of **3** had been carried out previously [12] although, to our knowledge, the complete structural details were not published. We have carried out structural characterization of compounds **1**–**4** in order to compare and analyze the data. The structure of compound **3** was repeated in order to have more structural information that would allow an analysis to be made; it is important to mention that the cell dimensions we obtained are different from those reported. Also, variable temperature multinuclear NMR studies were carried out for the same compounds. The dynamical behaviour is discussed in relation with the structural characteristics of each compound. Results are reported herein.

2. Results and discussion

2.1. Synthesis and spectroscopic characterization

The synthesis of substituted derivatives of $[H_4Ru_4(CO)_{12}]$ has been studied using different activation methods. Since thermal activation produces very low yields of the monosubstituted compounds $[H_4Ru_4(CO)_{11}L]$, for the synthesis of the phosphite derivatives (compounds **3** and **4**) and for the preparation of compound **2**, we used the same method that Aime et al. [8] activating the cluster with $[FeCp(CO)_2]$. This method though, does not produce satisfactory results for the preparation of compound **1** therefore trimethyl amine oxide was used in that case.

IR and NMR spectroscopic information for compounds **1**, **2** and **3** is given in Section 3 and in Tables 1 and 2. The data obtained for compound **4** is similar to what had been reported previously. The IR information shows that carbonyl stretching frequencies for compound **1** appear at higher values indicating a lower back donation from the metal atoms to the COs as had been observed in other cluster compounds containing fluorinated phosphine substituents [13]. A recent study pointed out that $P(C_6F_5)_3$ is not a π acid and is a very poor σ donor ligand [14] so the trend observed would have to be associated with the poor donor ability of the ligand towards the metal core.

The ^1H NMR spectrum of **1** shows a slightly broad doublet with a $J(^{31}P–^1H) = 7$ Hz while in the ^{31}P NMR spectrum, only a singlet is observed; the $^{31}P–^{19}F$ coupling observed in the non-coordinated phosphine is not observed in the cluster compound. It is important to point out that compound **1** is not stable in solution and after a few minutes, the spectrum shows signals due to the starting materials. This behaviour is in sharp contrast with the stability shown by compounds **2**–**4**.

2.2. Structural characterization

Molecular plots of compounds **1**, **2** and **4** are shown in Figs. 1–3 while some selected bond distances and angles are given in Table 3. As already pointed out, the structure of compound **3** had been carried out but not reported in detail therefore we repeated it in our laboratory in order to be able to compare the results with those of the other compounds we are interested in; the unit cell information we obtained is different from that described [15] so we believe this is another isomorphous crystalline form. The bond lengths and angles we obtained are also included in Table 3; they are not very different to those described in similar structures [16]; the molecular structure and numbering scheme of compound **3** is shown in Fig. 4.

Compounds **1**, **3** and **4** show the same general structure of a "Ru_4H_4" core of *D2d* geometry while in compound **2**, three of the hydrides bridge the edges adjacent to the ruthenium atom which is bonded to the phosphine in a similar pattern to that observed in diphosphine derivatives [7]. Additionally, while in the first three compounds the phosphorous ligands form P–Ru–Ru transoid angles of 172.26(3)°; compound **1**; 165.31(5)° and 166.13(5)°; compound **3** and 165.45(6)°; compound **4**; the distortion from the ideal *trans* angle is larger in **2** with a value of 159.03(5)° for the transoid P–Ru–Ru angle. The corresponding angles in $[H_4Ru_4(CO)_{10}L_2]$ are ca. 165° when $L = P(OEt)_3$ and ca. 171° when $L = PPh_3$. Puga et al. [7] suggested that the *Cs* structure observed in $[H_4Ru_4(CO)_{10}(diphos)]$ allows the H atoms to attain the maximum possible proximity to the electron rich metal atoms, i.e. those which are bonded to the phosphine with aliphatic substituents, better σ-donors than either phosphites or aryl substituted phosphines [14]. On

Table 1
Physical description and infrared data for compounds **1**–**3**

Compound	Colour	Melting point (°C)	IR ν(CO, cm^{-1}) (in hexane)
1	orange	154.4	2100(d), 2078(f), 2066(f), 2040(f), 2022(m), 2016(m), 1990(m)
2	orange red	127–129 (sublimes)	2094(d), 2088(d), 2066(m), 2058(f), 2032(m), 2026(m), 2008(m), 1990(d)
3	orange	104–105 (sublimes)	2096(d), 2068(f), 2058(f), 2030(f), 2016(m), 2008(f), 1994(d)

Table 2
^{1}H, ^{31}P, ^{19}F and ^{13}C NMR data for compounds **1**–**3**[a]

Compound	**1**	**2**	**3**[b]
^{1}H	−17.39(d, w)	2.24 (d, CH_3) $^{2}J(^{31}P–^{1}H) = 9.96$, 7.54(m, Ph), −17.51(s,w, *M–H)*	3.7308(d, Me) $^{3}J(^{31}P–^{1}H) = 12.16$ Hz; −17.737 (d, M–*H*) $J(^{31}P–^{1}H) = 2.145$ Hz)
^{31}P	−23.43(s)	5.99(s)	139.88(s)
$^{31}P(^{1}H)$	−23.47(m)	5.99 (m, w)	139.85(oq) $^{3}J(^{31}P–^{1}H) = 2.1$ Hz, $^{3}J(^{31}P–^{1}H) = 2.12$ Hz
^{13}C	aromatics: 125.34 (s, *Cp*), 126.23(s, *Cp*), 127.06(s, C*m*), 127.73(s, C*m*), 128.98(s, C*o*), 130.11(s, C*o*), 150.98(s, C*i*); CO's: 184.27(m), 185.66(s), 189.18(s), 190.04(s), 190.8(s), 192,58(s), 193.52(s)	methyl: 22.14(d), $^{1}J(^{31}P–^{13}C) = 33.83$ Hz	methyl: 52.68(d) $^{2}J(^{31}P–^{13}C) = 5.14$ Hz
		aromatics: δ (C*m*) = 129. 17(d) $^{3}J(^{31}P–Cm) = 10.04$ Hz; δ (C*o*) = 129.69(d), $^{2}J(^{31}P–Co) = 10.32$ Hz; δ (C*p*) = 131.24(d), $^{4}J(^{31}P–Cp) = 2.56$ Hz; δ (C*i*) = 137.67 (d), $^{1}J(^{31}P–Ci) = 49.13$ Hz carbonyls: δ (2A, 2B, 2C, 2E, 2F) = 193.21(s,w), δ (D) = 189.57(d), $^{3}J(^{31}P–^{13}C) = 9.41$ Hz	carbonyls: δ (2E) = 193.4, δ (4A) = 192.9, δ (2B/2C) = 191.8, δ (D) = 191.3(d), $^{3}J(^{31}P–^{13}C) = 9.23$ Hz), δ (2B/2C) = 189.1
$^{13}C(^{1}H)$	not obtained	D(Me) = 22.14(qdq), $^{1}J(^{13}C–^{1}H) = 127.66$ Hz, $^{3}J(^{13}C–^{1}$Hydride) = 2.1 Hz	methyl: 52.69(qd), $^{1}J(^{13}C–^{1}H) = 147.47$ Hz, $^{2}J(^{31}P–^{13}C) = 5.1$ Hz
^{19}F	F_{ortho}: $\delta = -127.35$(d, 6F) $^{3}J(^{19}Fo–^{19}Fm) = 18.66$ Hz F_{para}: $\delta = -146.01$ (tt, 3F) $^{3}J(^{19}Fp–^{19}Fm) = 20.77$ Hz, $^{4}J(^{19}Fp–^{19}Fo) = 5.1$ Hz F_{meta}: $\delta = -158.63$ (dd, 6F) $^{3}J(^{19}Fo–^{19}Fm) = 18.86$ Hz, $^{3}J(^{19}Fp–^{19}Fm) = 20.62$ Hz		

[a] Obtained in $COCl_3$.
[b] ^{13}C obtained at −30 °C.

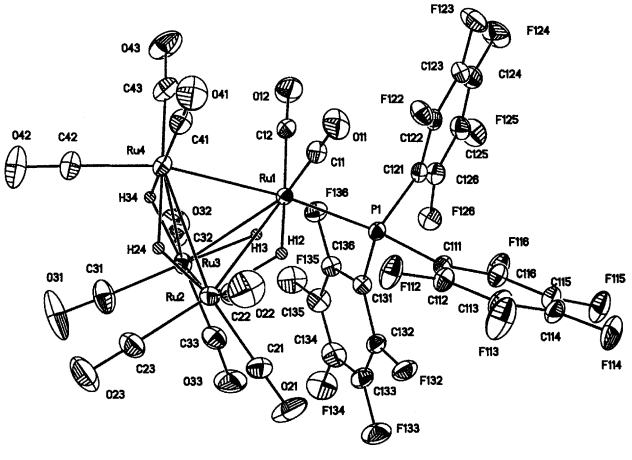

Fig. 1. Molecular structure, including numbering scheme, of $[H_4Ru_4(CO)_{11}P(C_6F_5)_3]$, compound **1**.

the other hand, the largest P–Ru–Ru transoid angles are found in the case of phosphines with large cone angles as it is in the case of **1** (see Table 3).

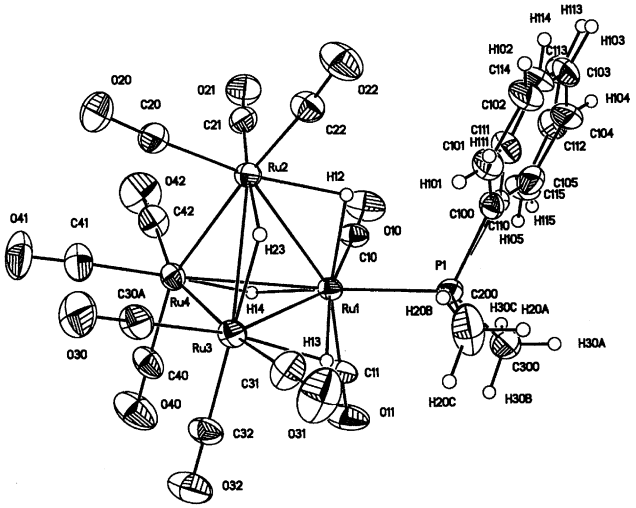

Fig. 2. Molecular structure, including numbering scheme, of $[H_4Ru_4(CO)_{11}PMe_2Ph]$, compound **2**.

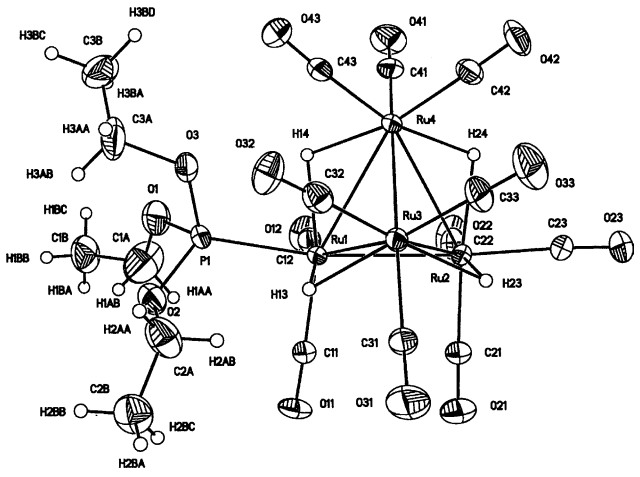

Fig. 3. Molecular structure, including numbering scheme, of $[H_4Ru_4(CO)_{11}P(OEt)_3]$, compound **4**.

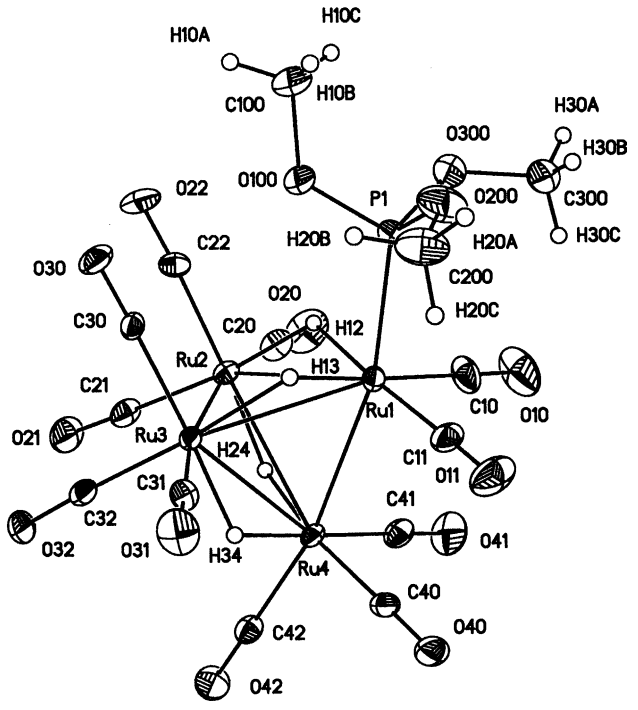

Fig. 4. Molecular structure, including numbering scheme, of $[H_4Ru_4(CO)_{11}P(OMe)_3]$, compound **3**.

Another characteristic of **2** that is worth pointing out is that it has the longest Ru–Ru long bond lengths of the 4 compounds, with an average value of 2.978 Å. Short Ru–Ru bond lengths are similar in all 4 compounds. Studies carried out on the systematic structural changes caused by different substituents in some transition metal clusters [9,10,17] have shown that there is some lengthening of metal–metal bonds *trans* and *cis* to the substituents. This is not the case in compounds **1**–**4**, probably due to the presence of the hydrides. Neither do we observe a direct relationship between cone angle of the phosphine and M–M bonds. Compound **1** which contains $P(C_6F_5)$ (Cone angle = 184°) does not show significantly different M–M bond distances from the other three compounds.

As expected, larger differences are found when comparing Ru–P distances. A highly significant trend of increasing Ru–P bond lengths with increasing donicity and/or size of the substituents has been observed [10] but no clear trend can be deduced in our small set of compounds. Values for Ru–P distances in compounds **1** and **2** are similar and significantly different from those in **3** and **4**. According to the QALE method [14], of the four phosphorus ligands used in our study, PMe_2Ph is the best σ-donor and $P(C_6F_5)_3$ is the worst but the Ru–P bonds in their corresponding compounds differ only by 0.018 Å while comparing the same values in compounds **2** and **4**, (with more similar σ-donor capacities; 10.5 versus 15.8); gives a difference of 0.0576 Å, a difference which can be a consequence of the larger cone angle of PMe_2Ph (122° versus 109°).

Metal carbonyl bonds show very similar values in all our compounds with Ru–C distances averaging to 1.902, 1.9002, 1.899 and 1.902 Å, respectively, for compounds **1**–**4**.

Table 3
Selected bond lengths (Å) and angles (°) for compounds **1**–**4**

Compound	**1**	**2**	**3**[a]	4
Bond lengths				
Ru(l)–Ru(2)	2.9532 (7)	2.9774 (7)	2.9531 (12); 2.9647 (12)	2.792 (1)
Ru(l)–Ru(3)	2.9605 (7)	3.0191 (10)	2.9427 (9); 2.9601 (9)	2.967 (2)
Ru(l)–Ru(4)	2.7841 (9)	2.9838 (7)	2.7873 (10); 2.7834 (9)	2.971 (1)
Ru(2)–Ru(3)	2.7834 (8)	2.9328 (7)	2.7921 (12); 2.7943 (13)	2.958 (1)
Ru(2)–Ru(4)	2.9582 (8)	2.7823 (7)	2.9668 (10); 2.9579 (10)	2.957 (1)
Ru(3)–Ru(4)	2.9417 (8)	2.7846 (8)	2.9568 (11); 2.9698 (12)	2.786 (1)
Ru(1)–P(1)	2.362 (1)	2.345 (1)	2.286 (2) 2.281 (2)	2.287 (2)
Bond angles				
P(1)–Ru(1)–Ru(2)	114.42 (4)	108.00 (4)	104.92 (5); 105.09 (5)	165.44 (6)
P(1)–Ru(1)–Ru(3)	110.74 (3)	106.15 (4)	107.35 (5); 105.64 (5)	105.81 (7)
P(1)–Ru(1)–Ru(4)	172.25 (3)	159.03 (4)	166.13 (5); 165.31 (5)	105.73 (6)

[a] There are two molecules in the asymmetric unit.

An analysis of intramolecular non-bonded distances in compound **1**, shows a close contact between two of the hydrides and two of the *ortho*-substituted fluorine atoms (H(12)–F(112) 2.44(6) Å and H(13)–F(136) 2.54(7) Å). These values are below the sum of the van der Waals radii [18].

M–H and C–F bonds have been considered as weak donors and weak acceptors, respectively, for the formation of hydrogen bonds [19]. However it has been shown that metal hydrides in polymetallic complexes can form hydrogen bonds if the hydrogen bond is not sterically hindered [20]. On the other hand, fluorine atoms in fluorobenzenes have also been observed to form C–H–F interactions [21]. Therefore a hydride–fluorine interaction seems plausible and we have evidence of its existence in another cluster compound [13]. It has to be pointed out that no evidence of such an interaction is observed in the solution NMR spectra of compound **1**.

2.3. Dynamics of compounds 1, 2 and 3

The VT NMR studies carried out in compound **4** and the similar PPh_3 and $AsPh_3$ derivatives [8], suggested that the hydrides are scrambling over the whole tetrahedron while the $Ru(CO)_3$ moieties exhibit a localized exchange. The ^{31}P and ^{1}H spectra of **4** at −120° were explained by the presence of one geometrical major isomer, probably the one observed in the solid state, and a less symmetrical set of two minor isomers of equal populations. The structures of these isomers were proposed imposing as a restriction that the phosphine ligand has to be transoid to a non-bridged metal–metal edge, as it is observed in the solid state of this compound. In order to observe whether the different substituents modified the dynamical behaviour of the derivatives, variable temperature NMR studies of compounds **1**, **2** and **3** were carried out. Due to some technical problems only compound **2** was analysed at temperatures between −120 and −90 °C. The lowest temperature used for the other two compounds was −90 °C.

A similar study in compound **1** showed a similar behaviour. Fig. 5 includes ^{1}H spectra of compound **1** obtained at 10° intervals from −90 to 100 °C. As mentioned previously, the ^{1}H spectrum of **1** at room temperature only shows a slightly wide doublet indicating the equivalence of the four hydrides; the doublet ($J(^{31}P–^{1}H) = 7.04$ Hz) becomes a wide singlet at 10 °C which at −20 °C changes to two wide signals which then split into a doublet each at −30 °C, these two signals have equal intensity with two different coupling constants to phosphorus (2.92 and 9.76 Hz), suggesting that the solution contains two isomers as a result of the hydride migration. These signals remain unchanged until −80° while at −90° both signals become wider and only one of them remains as a doublet ($J(^{31}P–^{1}H) = 3.2$ Hz). On the other hand, the ^{31}P spectra shows a singlet which remains constant at the whole temperature interval studied and, apart from a signal corresponding to the free phosphine, only two very small signals are observed at −90 °C. At this same temperature, the study of compound **4** reported shows in the ^{1}H spectrum two wide signals which split into seven signals at −120 °C. The ^{31}P NMR spectrum of **4** at −90 °C shows one major and one minor signals.

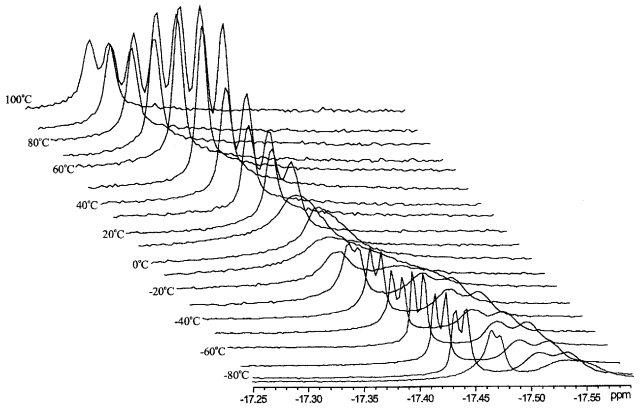

Fig. 5. Variable temperature (−90 to 100 °C) ^{1}H NMR spectra in the hydride region of $[H_4Ru_4(CO)_{11}P(C_6F_5)_3]$, compound **1**.

In the case of compound **2**, we could obtain the ^{1}H spectra at −120 °C and it shows two single wide signals and one wide doublet (Fig. 6). These signals become narrower when the spectrum is obtained at −110 °C and one of the wide single signal splits into a doublet and this pattern remains until −90 °C. The relative intensity of the signals is 1:1. At −90 °C one of the signals splits into a wide singlet and a doublet ($J = 29.83$ Hz) while the other signal splits into a doublet with a coupling constant value of 17.26 Hz. The relative intensities of the signals are 1:1:2. These also suggests the presence of three isomers: a major one, presumably with the structure observed in the solid state, and two minor isomers.

As expected, compound **3** shows very similar variable temperature NMR spectroscopic spectra to the ones reported for compound **4**, therefore suggesting a similar dynamical behaviour in both compounds. As mentioned above, Aime et al. proposed the different isomeric structures taking as a premise that they would always have the phosphine ligand transoid to a non-bridged metal–metal bond (Structures I, II and III in Scheme 1). The structure observed in compound **2** (Structure IV in Scheme 1), could mean this will not necessarily be true and that similar structures could be present, even if it is as minor isomers, for compounds **3** and **4**.

Another aspect that has to be pointed out is that in the spectra of compound **2**, the most intense signal, which we think corresponds to the structure observed in the solid state, shows a smaller $^{1}H–^{31}P$ coupling constant than the ones observed for the other isomers. This

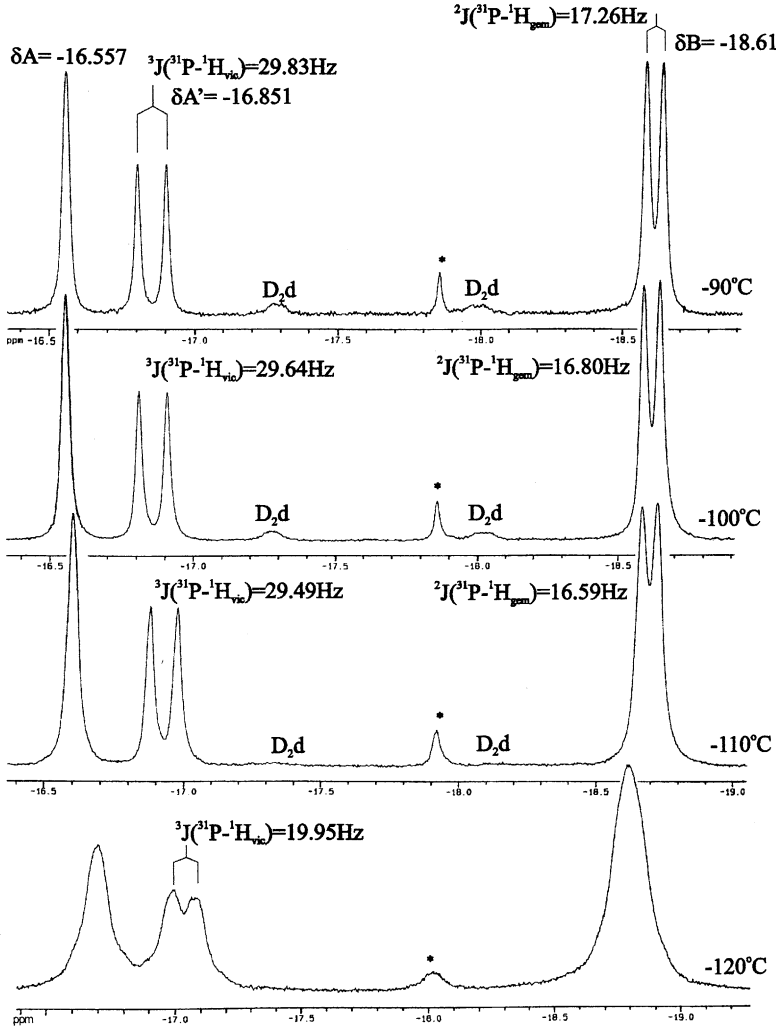

Fig. 6. Variable temperature (−120 to −90 °C) ^1H NMR spectra in the hydride region of $[H_4Ru_4(CO)_{11}PMe_2Ph]$, compound **2**.

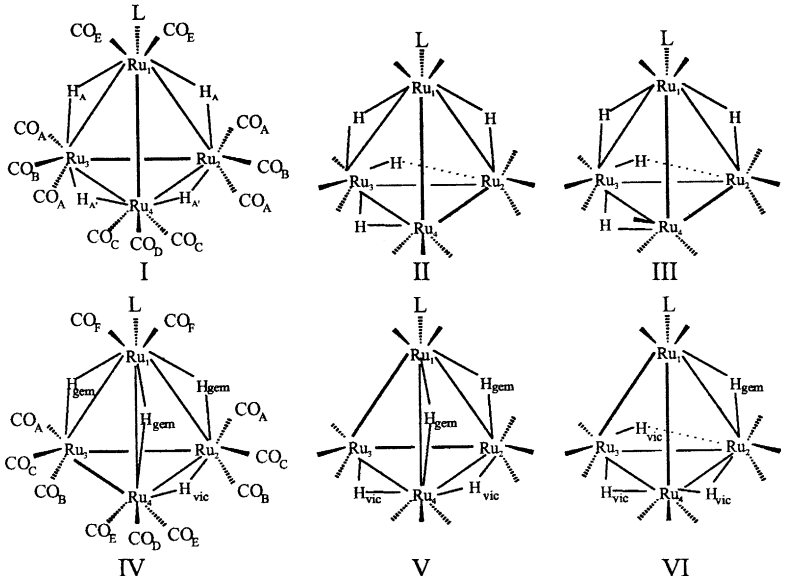

Scheme 1.

would mean that coupling constant values for some of the vicinal hydrides show larger values than the corresponding values for geminal hydrides. All three compounds show signals with different coupling constants. The values for **1** and **2** were already mentioned while in **3** we can observe signals with $J(^{31}P–^{1}H) = 11.7$ and 1.9 Hz. Structures I–VI have different numbers of vicinal and geminal hydrides and the sum of the different numbers of each in the different structures participating in the equilibrium could give as a result signals with different relative intensities and coupling constants.

With these points in mind we propose that the structures participating in the dynamical equilibrium in all 4 compounds are I, IV, V and VI in Scheme 1 with structure I (of *D2d* symmetry) as the major isomer in compounds **1**, **3** and **4** and structure IV (*Cs* symmetry) as the major isomer in the case of compound **2**.

3. Experimental

3.1. General procedures

All reactions and other manipulations were carried out under a nitrogen atmosphere using standard Schlenk techniques. All solvents were dried and distilled under a nitrogen atmosphere prior to use. Infrared spectra were recorded on a Pekin–Elmer 2000 spectrometer in hexane solutions. NMR spectra were obtained in a Jeol Eclipse 400 or a Bruker Avance^{TM} DPX 300 spectrometers, ^{1}H and ^{13}C spectra relative to $SiMe_4$ and ^{31}P relative to H_3PO_4, in $CDCl_3$ solutions. $[Ru_3(CO)_{12}]$ and the phosphines were purchased from Strem and Aldrich and were used without further purification. Me_3NO was also dried prior to use. $[H_4Ru_4(CO)_{12}]$ was prepared as reported [22].

3.2. Synthesis of $[H_4Ru_4(CO)_{11}(P(C_6F_5)_3)]$, compound 1

$[H_4Ru_4(CO)_{12}]$ (0.03 g; 0.04 mmol) and $P(C_6F_5)_3$ (0.0268 g, 0.05 mmol) were dissolved in 20 ml of dichloromethane. Me_3NO (0.5 eq., 0.0015 g) dissolved in acetonitrile (7.5 ml) was slowly added to the first solution kept at −10 °C and the solution was stirred for 1 h. The resulting solution is filtered through a column packed with silica and the solvent was then removed under vacuum. Orange crystals of **1** are obtained from a concentrated dichloromethane solution. Melting point: 154–155 °C. FAB for **1**: 1248. Yield: 32%. Infrared data: 2100(d), 2078(f), 2066(f), 2040(f), 2022(m), 2016(m), 1990(m). NMR Data. ^{1}H: −17.39 (d, w), ^{31}P: −23.43(s), $^{31}P(^{1}H)$: −23.47(m) ^{13}C: Aromatics: 125.34(s,*Cp*), 126.23(s, *Cp*), 127.06(s, C*m*), 127.73(s, C*m*), 128.98(s, C*o*), 130.11(s, C*o*), 150.98(s, C*i*); CO's: 184.27(m), 185.66(s), 189.18(s), 190.04(s), 190.8(s), 192,58(s), 193.52(s). ^{19}F data: F_{ortho}: $\delta = -127.35$(d, 6F) $^{3}J(^{19}Fo–^{19}Fm) = 18.66$ Hz F_{para}: $\delta = -146.01$(tt, 3F) $^{3}J(^{19}Fp–^{19}Fm) = 20.77$ Hz, $^{4}J(^{19}Fp–^{19}Fo) = 5.1$ Hz F_{meta}: $\delta = -158.63$(dd,6F) $^{3}J(^{19}Fo–^{19}Fm) = 18.86$ Hz, $^{3}J(^{19}Fp–^{19}Fm) = 20.62$ Hz (see Table 2).

3.3. Synthesis of $[H_4Ru_4(CO)_{11}(PMe_2Ph]$, compound 2

$[H_4Ru_4(CO)_{12}]$ (0.111 g; 0.15 mmol) and $[FeCp(CO)_2]_2$ (0.006 g; 0.015 mmol) were dissolved in 20 ml of cyclohexane and the suspension is placed in an ultrasound bath for 10 min. After that time PMe_2Ph (0.18 mmol) is added to the solution and the bath is heated to 42 °C for 2 h. The solvent is then evaporated to dryness and the residue purified by column chromatography using silica and a 7:3 heptane–dichloromethane solution. Orange red crystals were obtained from a concentrated dichloromethane solution. Melting point: 127–129 °C. FAB 854 amu. Microanalysis: C: 26.23% (26.7%), H: 1.71%(1.77). Yield: 44.18%. Infrared data: 2094(d), 2088(d), 2066(m), 2058(f), 2032(m), 2026(m), 2008(m),1990(d). NMR data: ^{1}H: 2.24(d, CH_3) $^{2}J(^{31}P–^{1}H) = 9.96$, 7.54(m, Ph), −17.51(s,w, M–*H*). ^{31}P: 5.99(s), $^{31}P(^{1}H)$: 5.99(m,w); ^{13}C: Methyl: 22.14(d), $^{1}J(^{31}P–^{13}C) = 33.83$ Hz, Aromatics: δ (C*m*) = 129.17(d) $^{3}J(^{31}P–Cm) = 10.04$ Hz; δ (C*o*) = 129.69(d), $^{2}J(^{31}P–Co) = 10.32$ Hz; δ (C*p*) = 131.24(d), $^{4}J(^{31}P–Cp) = 2.56$ Hz; δ (C*i*) = 137.67(d), $^{1}J(^{31}P–Ci) = 49.13$ Hz, Carbonyls: δ (2A, 2B, 2C, 2E, 2F) = 193.21(s,w), δ (D) = 189.57(d), $^{3}J(^{31}P–^{13}C) = 9.41$ Hz; $^{13}C(^{1}H)$: δ (Me) = 22.14(qdq), $^{1}J(^{13}C–^{1}H) = 127.66$ Hz, $^{3}J(^{13}C–^{1}H$hydride$) = 2.1$ Hz.

3.4. Synthesis of $[H_4Ru_4(CO)_{11}(P(OMe)_3]$ and $[H_4Ru_4(CO)_{11}(P(OEt)_3]$, compounds 3 and 4

$[H_4Ru_4(CO)_{11}L]$ ($L = P(OMe)_3$ and $P(OEt)_3$) were prepared following the procedure reported by Aime et al. [8]. Although using an ultrasound bath and 2 equivalents of the phosphite for each one of the cluster compound [8]. Yield of compound **3**: 32%; yield of compound **4**; 34.2%. Microanalysis for **3**: C: 20.94%(20.01), H: 1.60%(1.56). Microanalysis for **4**; C: 23.66%(23.14), H: 2.17%(2.17). FAB for **3**: 842; FAB for **4**: 882; Melting point for **3**: 104–105 °C (sublimes). Infrared data for **3**: 2096(d), 2068(f), 2058(f), 2030(f), 2016(m), 2008(f), 1994(d). NMR data for **3**: ^{1}H: 3.7308(d, Me) $^{3}J(^{31}P–^{1}H) = 12.16$ Hz; −17.737(d, M–*H*) $J(^{31}P–^{1}H) = 2.145$ Hz); ^{31}P: 139.88(s), $^{31}P(^{1}H)$: 139.85(oq) $^{3}J(^{31}P–^{1}H) = 2.1$ Hz, $^{3}J(^{31}P–^{1}H) = 2.12$ Hz; ^{13}C (obtained at −30 °C): Methyl: 52.68(d) $^{2}J(^{31}P–^{13}C) = 5.14$ Hz, Carbonyls: δ(2E) = 193.4, δ(4A) = 192.9, δ (2B/2C) = 191.8, δ (D) = 191.3(d, $^{3}J(^{31}P–^{13}C) = 9.23$ Hz), δ (2B/2C) = 189.1; $^{13}C(^{1}H)$: Methyl: 52.69(qd), $^{1}J(^{13}C–^{1}H) = 147.47$ Hz, $^{2}J(^{31}P–^{13}C) = 5.1$ Hz.

3.5. Crystallographic studies

Crystals of **1**–**4** were grown from CH_2Cl_2 solutions. Details of the data collection and structure refinement

Table 4
Data collection parameters and structure refinement procedures for compounds **1**–**4**

Compound	**1**	**2**	**3**	**4**
Formula	$C_{29}H_4F_{15}O_{11}PRU_4$	$C_{19}H_{15}O_{11}PRU_4$	$C_{14}H_{13}O_{14}PRU_4$	$C_{17}H_{19}O_{14}PRu_4$
Molecular weight	1248.57	854.56	840.49	882.57
Crystal size (mm)	$0.5 \times 0.4 \times 0.4$	$0.45 \times 0.31 \times 0.11$	$0.3 \times 0.4 \times 0.4$	$0.5 \times 0.4 \times 0.4$
Crystal color and habit	orange prism	red orange blocks	red orange prisms	red orange blocks
System	monoclinic	monoclinic	triclinic	triclinic
Space group	$P2_1/n$	$P2_1/C$	$P\bar{1}$	$P\bar{1}$
a (Å)	12.701(3)	9.803(2)	11.241(2)	9.821(2)
b (Å)	13.192(3)	12.460(2)	13.607(3)	11.049(2)
c (Å)	21.560(4)	22.300(4)	16.648(3)	14.195(3)
α (°)	90	90	80.02(3)	83.21(3)
β (°)	90.13(3)	100.26(3)	79.36(3)	88.60(3)
γ (°)	90	90	86.94(3)	66.47(3)
V (Å^3)	3612.4(14)	2680.3(8)	2464.2(8)	1401.9(5)
z	4	4	4	2
ρ_{calc} (Mg m^{-3})	2.296	2.118	2.266	2.091
$F(000)$	2368	1632	1600	848
γ (Mo Kα) (Å)	0.71073	0.71073	0.71073	0.71073
μ (Mo Kα) (mm^{-1})	1.820	2.321	2.531	2.230
2θ range (°)	4–50	4–50	4–50	4–50
Temperature (K)	293(2)	293(2)	293(2)	293(2)
h_{min}/h_{max}	−15/0	0/11	−13/13	−11/11
k_{min}/k_{max}	0/15	0/14	−15/16	−12/13
l_{min}/l_{max}	−25/25	−26/26	0/19	0/16
Measured reflections collected	6651	6124	7716	4912
Observed reflections ($F > 4\sigma(F)$)	5123	4048	6621	4172
R_{int}	0.0177	0.001		
GOF on F^2	0.986	1.083	1.074	1.047
$R_1[F > 4\sigma(F)]$	0.0311	0.0384	0.0324	0.0588
wR_2 (on F^2 all data)[a]	0.08940	0.1057	0.0819	0.2060

procedures are summarized in Table 4. Data sets were collected in an Enraf-Nonius CAD4 diffractometer. The samples were mounted in capillary tubes. All structures were solved by direct methods (SHELXS-93) [23]. All non-hydrogen atoms were found in Fourier maps and refined anisotropically. Hydrogen atoms from phenyl and methyl groups were fixed in idealized positions and their positions refined. In the case of compounds **1**, **2** and **3**, hydrogen atoms of the hydrides were localized in Fourier maps and their coordinates refined. In the case of compound **2**, there is an occupational disorder in the phenyl ring of the phosphine so occupancy was refined yielding a 51% and 49% occupancy for each position. After this refinement, the carbon atoms of the ring were successfully refined anisotropically.

4. Supplementary

Crystallographic data for the structural analysis have been deposited with the Cambridge Crystallographic Data Centre, CCDC Nos.194936–194939. Copies of the information may be obtained free of charge from The Director, CCDC, 12 Union Road, Cambridge CB2 1EZ, UK (fax: +44-1223-336063; e-mail: deposit@ccdc.cam.ac.uk or www: http://www.ccdc.cam.ac.uk).

Acknowledgements

M.G.B.L. thanks Conacyt for the award of a grant. Thanks are given to Marco Antonio Leyva and Víctor M. González for their assistance with the X-ray structures and NMR spectra, respectively.

References

[1] R.K. Pomeroy, in: E.W. Abel, F.G.A. Stone, G. Wilkinson (Eds.), Comprehensive Organometallic Chemistry II, vol. 7, Pergamon Press, Oxford, 1995, p. 845.
[2] M. Bianchi, G. Menchi, U. Matteoli, F. Piacenti, J. Organomet. Chem. 451 (1993) 139.
[3] S. Bhaduri, K. Sharma, D. Mukesh, J. Chem. Soc., Dalton Trans. (1993) 1191.
[4] A.G. Orpen, R.K. McMullen, J. Chem. Soc., Dalton Trans (1983) 463.
[5] M.I. Bruce, E. Horn, O.B. Shawkataly, M.R. Snow, E.T. Tiekink, M.L. Williams, J. Organomet. Chem. 316 (1986) 187.
[6] J.R. Shapley, S.I. Richter, M.R. Churchill, R.A. Lashewycz, J. Am. Chem. Soc. 99 (1977) 7384.
[7] J. Puga, A. Arce, D. Braga, N. Centritto, F. Grepioni, R. Castillo, J. Ascanio, Inorg. Chem. 26 (1987) 867.

[8] S. Aime, M. Botta, R. Gobetto, L. Milone, D. Osella, R. Gellert, E. Rosenberg, Organometallics 14 (1995) 3693.
[9] K. Biradha, V.M. Hansen, W.K. Leong, R.K. Pomeroy, M.J. Zaworotko, J. Clust. Sci. 11 (2000) 285.
[10] D.H. Farrar, E.V. Grachova, A. Lough, C. Patirana, A.J. Poë, S.P. Tunik, J. Chem. Soc., Dalton Trans. (2001) 2015.
[11] D.H. Farrar, A.J. Poë, Y. Zheng, J. Am. Chem. Soc. 116 (1994) 6252.
[12] Footnote 24 in R. Wilson, R.J. Bau, J. Am. Chem. Soc. 98 (1976) 4687.
[13] G. Sánchez-Cabrera, Ph. D. Thesis. Cinvestav-IPN, 2001.
[14] A.L. Fernandez, M.R. Wilson, A. Prock, W.P. Giering, Organometallics 20 (2001) 3429.
[15] Cell dimensions of $[H_4Ru_4(CO)_{11}P(OMe)_3]$ reported in Ref. [12]: triclinic, $P\ -1$, $a = 13.69$, $b = 9.13$, $c = 11.26$ Å, $\alpha = 116$, $\beta = 93.2$, $\gamma = 97.1°$, $Z = 2$.
[16] R.D. Wilson, S. Miau Wu, R.A. Love, R. Bau, Inorg. Chem. 17 (1978) 1271.
[17] R.A. Burrow, D.H. Farrar, J. Hao, A. Lough, O. Mourad, A.J. Pôe, Y. Zheng, Polyhedron 17 (1998) 2907.
[18] J.E. Huheey, E.A. Keiter, R.L. Keiter, Inorganic Chemistry. Principles of Structure and Reactivity, 4th ed., Harper Collins College Publishers, New York, p. 292.
[19] G.R. Desiraju, Acc. Chem. Res. 35 (2002) 565.
[20] D. Braga, F. Grepioni, G.R. Desiraju, Chem. Rev. 98 (1998) 1375, and references therein.
[21] V.R. Thalladi, H.C. Weiss, D. Bläser, R. Boese, A. Nangia, G.R. Desiraju, J. Am. Chem. Soc. 120 (1998) 8702.
[22] M.I. Bruce, M.L. Williams, Inorg. Synth. 28 (1990) 219.
[23] G.M. Sheldrick, SHELX-93 Program for Crystal Structure Refinement. Institut fur Anorganische Chemie der Universität, Göttingen, Germany, 1993;
G.M. Sheldrick, SHELXS-86 Program for Crystal Structure Refinement. Institut fur Anorganische Chemie der Universität, Göttingen, Germany, 1993.